Marine Life Science & Technology
https://doi.org/10.1007/s42995-024-00222-4

RESEARCH PAPER

Deep learning-based fishing ground prediction with multiple environmental factors

Mingyang Xie[1] · Bin Liu[1,2] · Xinjun Chen[1,3,4,5]

Received: 30 June 2023 / Accepted: 7 February 2024

Abstract

Improving the accuracy of fishing ground prediction for oceanic economic species has always been one of the most concerning issues in fisheries research. Recent studies have confirmed that deep learning has achieved superior results over traditional methods in the era of big data. However, the deep learning-based fishing ground prediction model with a single environment suffers from the problem that the area of the fishing ground is too large and not concentrated. In this study, we developed a deep learning-based fishing ground prediction model with multiple environmental factors using neon flying squid (*Ommastrephes bartramii*) in Northwest Pacific Ocean as an example. Based on the modified U-Net model, the approach involves the sea surface temperature, sea surface height, sea surface salinity, and chlorophyll *a* as inputs, and the center fishing ground as the output. The model is trained with data from July to November in 2002–2019, and tested with data of 2020. We considered and compared five temporal scales (3, 6, 10, 15, and 30 days) and seven multiple environmental factor combinations. By comparing different cases, we found that the optimal temporal scale is 30 days, and the optimal multiple environmental factor combination contained SST and Chl *a*. The inclusion of multiple factors in the model greatly improved the concentration of the center fishing ground. The selection of a suitable combination of multiple environmental factors is beneficial to the precise spatial distribution of fishing grounds. This study deepens the understanding of the mechanism of environmental field influence on fishing grounds from the perspective of artificial intelligence and fishery science.

Keywords Deep learning · Center fishing ground · Multiple environmental factors · Temporal scales · U-Net · *Ommastrephes bartramii*

Special Topic: Fishery Science & Technology.

Edited by Xin Yu.

✉ Bin Liu
bliu@shou.edu.cn

✉ Xinjun Chen
xjchen@shou.edu.cn

1 College of Marine Sciences, Shanghai Ocean University, Shanghai 201306, China

2 Key Laboratory of Marine Ecological Monitoring and Restoration Technologies, Ministry of Natural Resources, Shanghai 200137, China

3 Key Laboratory of Oceanic Fisheries Exploration, Ministry of Agriculture and Rural Affairs, Shanghai Ocean University, Shanghai 201306, China

4 National Engineering Research Center for Oceanic Fisheries, Shanghai Ocean University, Shanghai 201306, China

5 Key Laboratory of Sustainable Exploitation of Oceanic Fisheries Resources, Ministry of Education, Shanghai Ocean University, Shanghai 201306, China

Introduction

Fishing ground prediction represents a crucial subject within fishery research. Precisely forecasting the location of fishing grounds holds immense significance in enhancing fishing yield and conserving fuel (Chen 2022). The spatial distribution of oceanic economic species exhibits a close association with their habitat (Chen et al. 2023; Gao et al. 2020; Huang et al. 2021). Prior studies have demonstrated that sea surface temperature (SST) exerts the greatest influence on fishing ground distribution (Alabia et al. 2016a). Alongside SST, other marine environmental factors, such as sea surface height (SSH), sea surface salinity (SSS), and chlorophyll a (Chl. *a*), display varying degrees of impact on fishing ground distribution (Alabia et al. 2015; Mustapha et al. 2009; Skogen et al. 2018). These marine environmental factors exhibit significant interannual variability, attributable to the influence of ocean climate. Consequently, a complex, dynamic, and integrated process of environmental

Published online: 29 April 2024

field changes emerges, leading to the formation of fishing grounds. Furthermore, a strong temporal and spatial correlation exists among different environmental factors. With the continuous advancement of space technology, sensor technology, and fishing gear technology, ocean remote sensing and fisheries have entered the era of big data (Li et al. 2020). Traditional methods encounter considerable challenges in effectively mining valuable information and establishing reliable prediction models in the face of complex and massive data. In contrast, deep learning has emerged as an application in ocean remote sensing and fisheries (Allken et al. 2021; Kroodsma et al. 2018; Li et al 2020; Xie et al. 2024). Deep learning-based fishing ground prediction models have become a promising avenue of research.

Deep learning has achieved notable success in addressing the challenges of processing image big data in various domains (Landy et al. 2022; Reichstein et al. 2019). The issue of fishing ground prediction may be regarded as a spatially correlated regression problem between the environmental field and fishing ground distribution within a specific time period. The comprehensive environmental field can be seen as a combination of different-dimensional environmental fields. The U-Net model, a classic deep learning network model for image semantic segmentation, excels in handling multi-dimensional spatial features. By employing fully convolutional neural network layers, it may integrate shallow and deep features of images while accurately estimating pixel categories and preserving the original resolution scale as much as possible (Ronneberger et al. 2015). Currently, this network has demonstrated favorable outcomes in ocean remote sensing and fisheries, including environmental monitoring (Liu et al. 2019, 2022), environmental forecasting (Zheng et al. 2020), and fishing ground prediction (Xie et al. 2024). In our previous research, we achieved real-time fishing ground prediction based on deep learning (Xie et al. 2024). However, the deep learning fishing ground prediction model constructed solely using the sea surface temperature (SST) factor faced challenges, such as excessive center fishing ground area and dispersed fishing ground distribution. To address this issue, we made improvements to the U-Net model by incorporating multiple environmental factors. We arranged sea surface height (SSH), sea surface salinity (SSS), and chlorophyll a (Chl *a*) in different channels of each input factor according to the temporal sequence. Additionally, we designed various environmental factor combination cases to investigate the differences in model outcomes and the improvement in the concentration of fishing ground distribution. In this study, we selected the neon flying squid (*Ommastrephes bartramii*) in the northwestern Pacific Ocean as our research case.

Ommastrephes bartramii is an important economic cephalopod species in the northwestern Pacific Ocean. Since its development and utilization by China in 1993, the annual yield has remained stable between 60,000 and 100,000 tons, making it a crucial target species for China's offshore fisheries (Chen et al. 2008). Among the oceanic environmental factors that affect pelagic economic species, SST is one of the most significant factors (Chande et al. 2021). The spatial variation in *Ommastrephes bartramii* fishing grounds is highly susceptible to SST and exhibits considerable changes (Yu et al. 2019). Additionally, SSH, SSS, and Chl. *a* also influence the distribution of fishing grounds (Alabia et al. 2015; Yatsu et al. 2000), and these factors often interact in a comprehensive manner. Therefore, in this study, we employed SST, SSH, SSS, and Chl. *a* as input factors and the distribution of center fishing grounds as the output factor of comprehensive environmental conditions. We constructed five different temporal scales and seven combinations of multiple environmental factors using data from July to November spanning the years 2002–2019. We employed an improved U-Net model to build a real-time fishing ground prediction model for *Ommastrephes bartramii* and investigated the impact of different temporal scales and combinations of multiple environmental factors on the model's performance. We compared the results with previous studies that focused on single factors and analyzed the importance of environmental factors during different time periods.

Materials and methods

Data

The commercial fisheries data were provided by the Chinese Squid-Jigging Technology Group at Shanghai Ocean University. The study area is the traditional fishing ground of *Ommastrephes bartramii* in the Northwest Pacific Ocean, bounded by 36°N to 48°N and 145°E to 165°E (Fig. 1). The fishery data comprise fishing dates and locations with longitude and latitude, the number of fishing vessels and the total catch recorded daily. The data collection spanned from July to November, covering the years 2002–2020.

The environmental data consisted of sea surface temperature (SST), sea surface height (SSH), sea surface salinity (SSS), and chlorophyll *a* (Chl. *a*). The SST data were obtained from the OceanWatch of the National Oceanic and Atmospheric Administration (NOAA, https://oceanwatch.pifsc.noaa.gov/) with a spatial scale of 0.05°. The SSH, SSS and Chl. *a* data were obtained from the University of Hawaii (http://apdrc.soest.hawaii.edu/data). The spatial scale for SSH and SSS data was 0.25°, whereas the Chl. *a* data were 4 km. The temporal scale for all environmental data was daily.

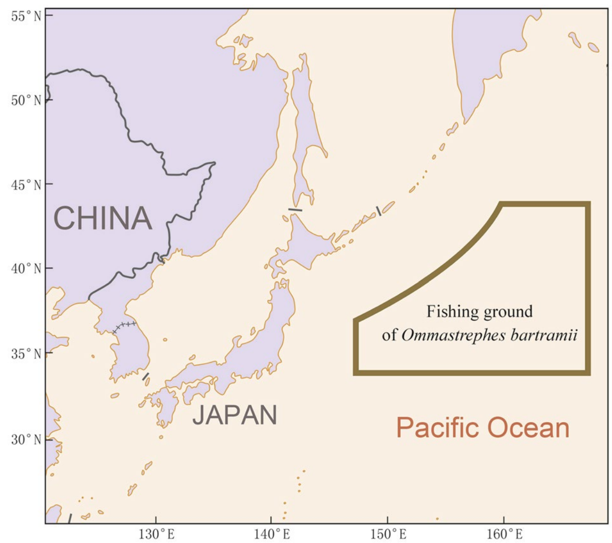

Fig. 1 Distribution of *Ommastrephes bartramii* fishing ground in the Northwest Pacific Ocean

Definition of the fishing ground

The previous study indicates a close correlation between the spatiotemporal distribution of *Ommastrephes bartramii* and changes in environmental factors, making use of the suitability range of environmental factors as the basis for identifying fishing grounds (Yu et al. 2017). Even when there is little or no catch at a particular site in a given period, scientific research surveys are still conducted. Due to constraints, such as time, manpower, and fuel costs, however, data for distant water fisheries cannot be sampled and surveyed at regular fishing grounds for each year, as is done with scientific research surveys. Information on the location and catch of sites in distant water fisheries is influenced by various factors, such as the maximum carrying capacity of fishing vessels, inter-fleet competition, and sea conditions. Therefore, distant water fisheries data, driven by commercial and economic purposes, exhibit strong randomness and incompleteness, referred to as *presence-only* data (Lei 2016). This implies that recorded fishing sites indicate the presence of catches, but unrecorded fishing sites do not represent the absence of catches. This leads to significant interannual differences in defining the suitability range of environmental factors for fishing grounds.

To address the presence-only issue, this study adopts the union of the suitability ranges of environmental factors for each year from 2002 to 2020 to represent the center fishing ground. To standardize the spatial and temporal scales of each environmental factor, the spatial scale was set at 0.25°, and temporal scales were set at five intervals of 3, 6, 10, 15, and 30 days. The previous study demonstrates that, at different temporal scales for *Ommastrephes bartramii*, there are noticeable differences in the suitability range of environmental factors (Yu et al. 2019). Therefore, different treatments were applied when defining center fishing grounds, taking into account different periods. As an example, for a temporal scale of a 30-day period, SST range for each month (July, August, …, and November) is defined as the historical minimum and maximum values for all years from 2002 to 2020. For a temporal scale of a 15-day period, SST range for each half month (1st half July, 2nd half July, …, and 2nd half November) is defined in the same way. Other environmental factors in different periods as above.

The resource abundance index, such as CPUE in the fishing ground, exhibits a considerable degree of dispersion, with relatively concentrated high index values (Table 1). Utilizing this characteristic, we used the quartile method to classify fishing ground types based on the environmental factor range corresponding to the resource abundance index for each period (Song et al. 2022). The environmental factor range with index values exceeding the upper quartile is defined as the center fishing ground, labeled as 1, whereas the remaining range is classified as the non-center fishing ground, labeled as 0. Since the distribution of fishing grounds is collectively influenced by each environmental factor, we defined the intersection of center fishing grounds under each individual environmental factor as the ultimate center fishing ground, whereas others are defined as non-center fishing grounds.

Catch, effort, and catch per unit effort (CPUE) are commonly used as resource abundance indices in fishing grounds (Tian et al. 2009). Through analysis, we observed that catch exhibits statistically significant differences in cases with varying temporal and spatial scales for each period (Table 1). Among the different indices, quartile analysis with catch proves to be more effective in defining the center fishing ground. Consequently, the catch index is selected as the resource abundance index.

Normalization and invalid value handling

To improve the fitting efficiency of the deep learning model, the environmental data are normalized to 0–1, and the calculation formula is shown as follows:

Table 1 Comparison of characteristics of different abundance indexes

Abundance index	Catch/t	Effort/vessel	CPUE/(t/v)
Minimum value	0.001	1	0.001
Maximum value	1047	203	5.158
Magnitude difference	10^6	10^2	10^3

$$x = \frac{x_i - x_{\min}}{x_{\max} - x_{\min}}, \tag{1}$$

where x is the normalized value of the sample, x_i is the original value, and $x_{\max}$ and $x_{\min}$ are the maximum and minimum values of the samples, respectively. All invalid values are replaced with − 1.

Prediction model and case design

The fishing ground prediction model (Fig. 2) is based on the U-Net model (Ronneberger et al. 2015). The U-Net model uses a fully convolutional architecture and consists of two paths, encoding and decoding. The encoding path reduces the spatial size and extracts high-level feature information for accurate classification. It is composed of convolutions with rectified linear unit (ReLU) activation and max-pooling processes. The decoding path combines abstracted and high-resolution features using a sequence of upsampling and concatenations. It is composed of upsampling processes and convolutions with ReLU activation. Pixel-level predictions are made in the final part of the network, enabling both classification and regression. As shown in Fig. 2, the model has three upsampling layers, three max-pooling layers, two dropout layers, and three skip connections. The max-pooling and convolution layers were applied with strides of 2 and 1, respectively. After pooling, the sample size is reduced to $1/2 \times 1/2$, whereas the number of feature channels remains unchanged. The ReLU activation adds nonlinearity to the output of the convolutional layer and enhances the nonlinear characteristics of feature learning. The primary reason for using max pooling is that it may reduce the calculation amount, improve the receptive field of convolutions, achieve learned features of multiple scales, and increase the model's robustness to noise and clutter. The pre-experimental results showed severe overfitting of the model without specific processing. Therefore, we added the SpatialDropout2D layer (Tompson et al. 2015), which is helpful for convolution layers, to the two and three levels of convolutions. The dropout rate of the SpatialDropout2D layer is set to 0.75 in this study. Since the model's aim is binary classification, center fishing ground or not, the last convolutional layer uses sigmoid activation. For the same reason, the model's loss function is binary cross-entropy (Lin et al. 2017).

To explore the differences in model performance resulting from different combinations of environmental factors, seven cases were designed (Table 2), each with five different temporal scales: 3 days, 6 days, 10 days, 15 days, and 30 days. Previous studies have confirmed that sea surface temperature (SST) is a crucial environmental factor for fishing ground prediction, so SST is included in all combination cases (Yatsu et al. 2000). The distribution maps of different environmental factors are sequentially stored in different channels and merged into a single input factor, with the fishing ground distribution as the output factor. Taking the example of a 3-day temporal scale in Case 1, the image has a pixel size of 48×80, four channels, and a sample size of 900 (Fig. 2).

After the process of encoding and decoding, the size of the sample remains the same, and the image features are effectively extracted. The model can make pixelwise predictions, from marine environmental factors to fishing grounds. Finally, we constructed this model to predict the fishing ground with multiple environmental factors.

Case implementation and evaluation

The overall accuracy (OA) is used to evaluate the quality of the model. OA refers to the proportion of correctly predicted pixels in all pixels. In addition, the precision, recall, and F1 score of the prediction results are usually calculated to test the quality of the model. Precision denotes the proportion of correct predictions in all the predicted fishing ground pixels. Recall refers to the proportion of center fishing ground pixels that are correctly predicted. There is a trade-off relationship between precision and recall, so the F1 score is calculated to comprehensively consider the model's performance, which is the harmonic mean of precision and recall. The metrics are calculated as follows:

$$\text{Overall accuracy}: \text{OA} = \frac{N_{\text{TP}} + N_{\text{TN}}}{N_{\text{TP}} + N_{\text{TN}} + N_{\text{FP}} + N_{\text{FN}}} \times 100\% \tag{2}$$

$$\text{Precision}: P = \frac{N_{\text{TP}}}{N_{\text{TP}} + N_{\text{FP}}} \tag{3}$$

$$\text{Recall}: R = \frac{N_{\text{TP}}}{N_{\text{TP}} + N_{\text{FN}}} \tag{4}$$

$$F1 = \frac{2PR}{P + R} = \frac{2N_{\text{TP}}}{2N_{\text{TP}} + N_{\text{FP}} + N_{\text{FN}}}, \tag{5}$$

where N_{TP} (TP stands for true positive) is the number of correctly predicted center fishing ground pixels, N_{TN} (TN stands for true negative) is the number of correctly predicted non-center fishing ground pixels, N_{FP} (FP stands for false positive) is the number of falsely predicted center fishing ground pixels, and N_{FN} (FN stands for false negative) is the number of falsely predicted non-center fishing ground pixels.

We built the fishing ground prediction model with TensorFlow 2.4.1 in Python 3.7. The model is run on the NVIDIA GeForce RTX 2080 Ti graphics processing unit, and the operating system is Ubuntu. We take the environmental factor data of 36°–48°N and 145°–165°E in the Northwest Pacific Ocean from 2002 to 2020 as the input, and make a one-to-one correspondence with the ground truth

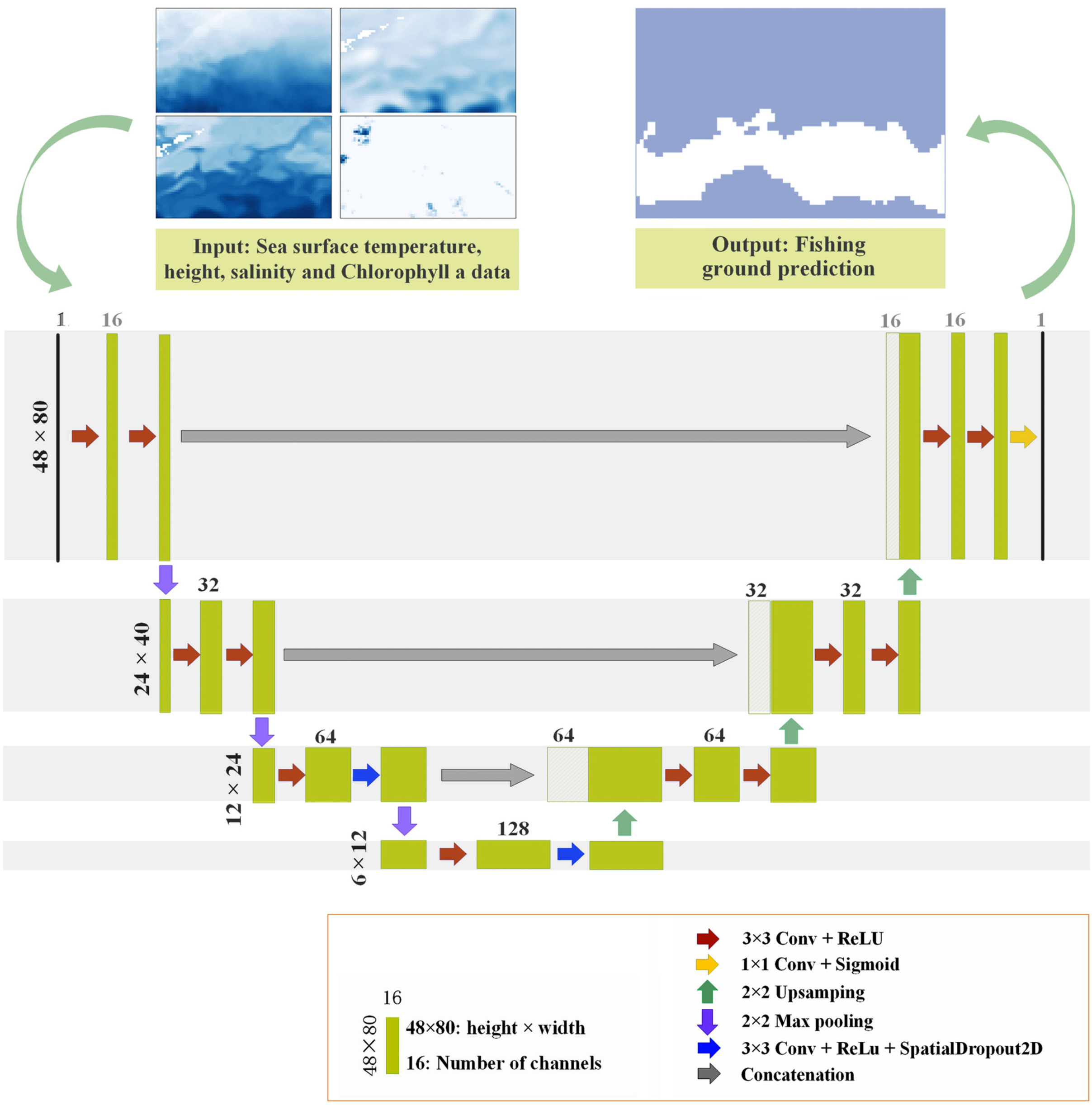

Fig. 2 Architecture of the fishing ground prediction model for multiple environmental factors (the example is used for Case 1 with a temporal scale of 3 days)

Table 2 Case design for multiple environmental factor combinations

Cases types	SST	SSH	SSS	Chl. *a*
Case 1	*	*	*	*
Case 2	*		*	*
Case 3	*	*		*
Case 4	*	*	*	
Case 5	*	*		
Case 6	*		*	
Case 7	*			*

*Indicates the factors included in the cases

of the center fishing ground. Then, a dataset with multiple temporal scales and environmental factor combinations is constructed. In this dataset, we select samples from 2002 to 2019 as training samples. These training samples are randomly divided into training and validation sets at a ratio of 4:1. The fishing ground prediction model is fit on the training set, and the optimal parameters for model fitting are selected with the validation set. Finally, the samples in 2020 are selected as the testing set.

Application effectiveness evaluation

Actual catch data usually consist of discrete sites containing high- and low-value information. The application effectiveness of the model is evaluated by calculating the proportion of actual catch within the predicted center fishing ground. This is expressed as the catch coverage rate (CCR). Previous research has shown that models constructed solely using SST have good CCR, but the area proportion of the center fishing ground (AP_{CFG}) is too large, resulting in a lack of concentration in the predicted center fishing ground. Therefore, we propose the application effect index of the fishing ground (AEI_{FG}) to evaluate the application effectiveness of the prediction model, calculated as follows:

$$AEI_{FG} = \frac{CCR}{AP_{CFG}};$$

here, a higher CCR and a smaller AP_{CFG} result in a higher application effect index of the fishing ground (AEI_{FG}). This indicates better application effectiveness of the prediction model.

Results

Model results and evaluation of different cases

From the loss curves of the training and validation sets of all models at different temporal scales (Fig. 3), all cases achieved a satisfactory fit within the 300-epoch limit. Furthermore, the inclusion of regularization (two layers of SpatialDropout2D) allows the models to delay the occurrence of overfitting as much as possible. Among all the cases, the minimum loss values on the training set ranged from 0.06 to 0.26, whereas the minimum loss values on the validation set ranged from 0.09 to 0.27. The optimal accuracy on the validation set ranged from 88.43% to 96.37%, fluctuating between 87 and 92% after overfitting (Fig. 4).

To assess the performance of the fishing ground prediction model with multiple environmental factors at different temporal scales, it was tested on the testing set using overall accuracy (OA) and F1 score as evaluation metrics. From the model performance evaluation (Fig. 5), the trends in OA and F1 scores were consistent among different environmental factor combination cases. There were significant differences in model performance among the different cases. Case 7 exhibited better performance across all temporal scales compared to other cases, with the 30-day temporal scale achieving the highest accuracy

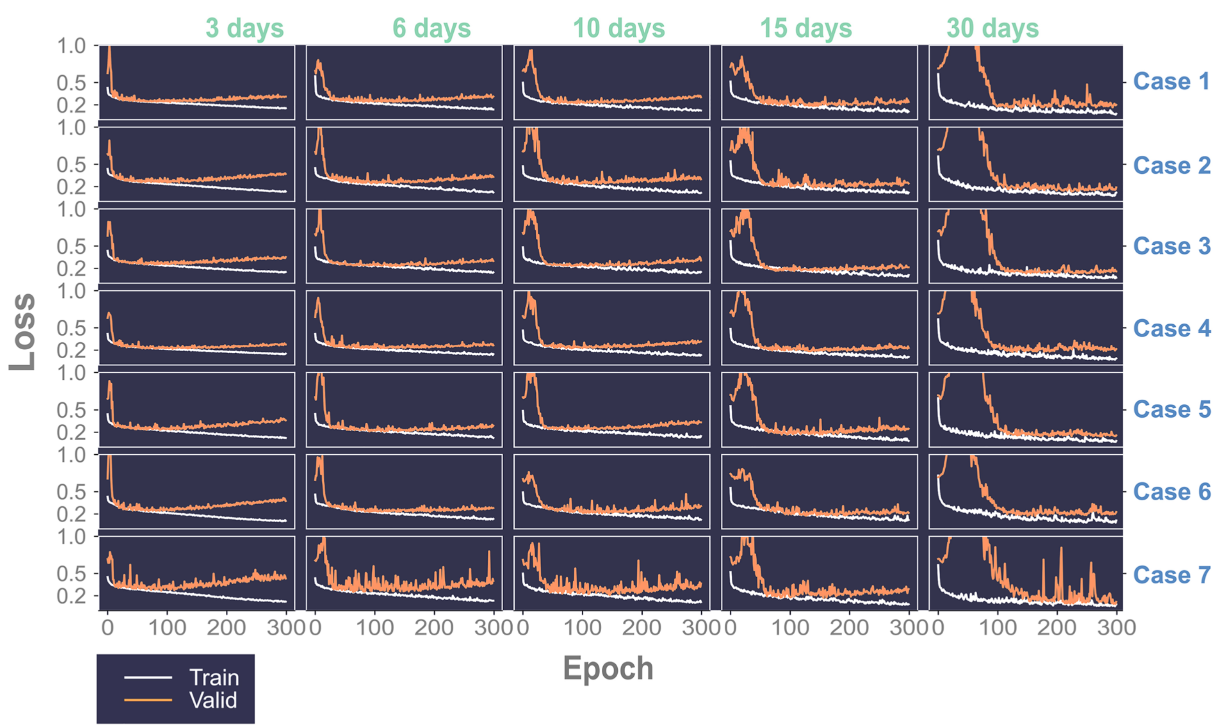

Fig. 3 Loss curves of the training and validation set of the fishing ground prediction model with multiple environmental factors at different temporal scales

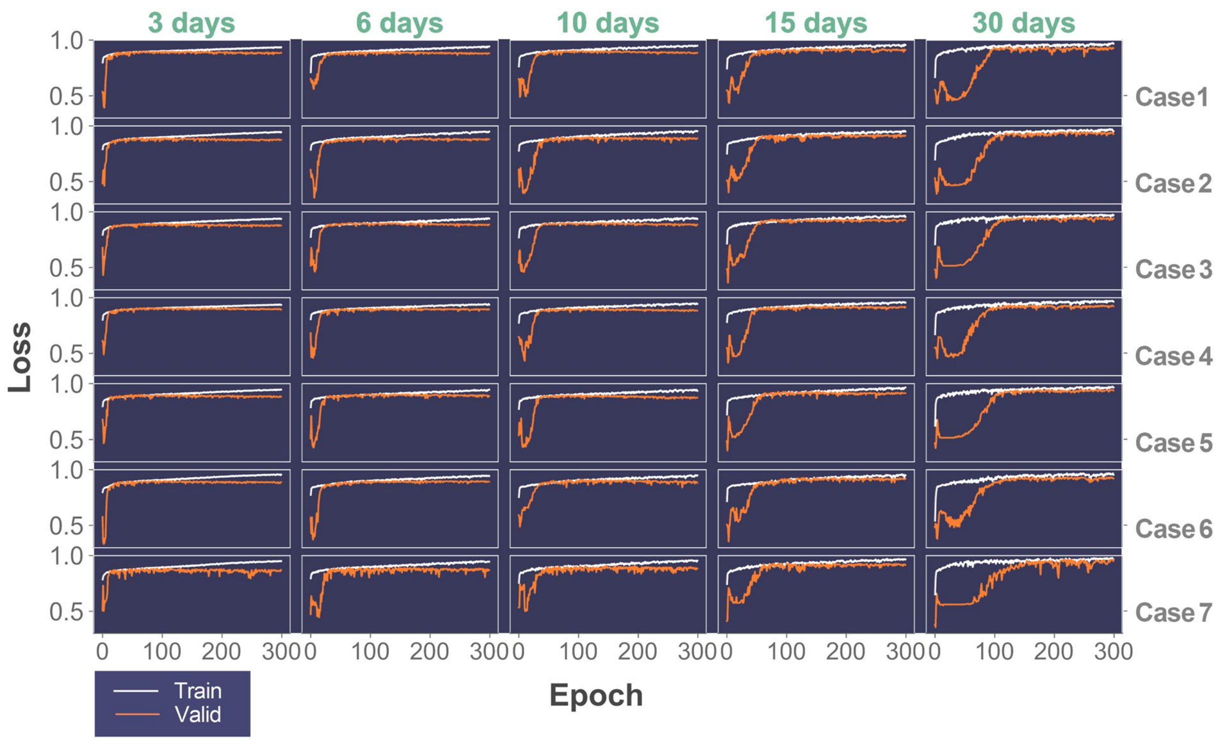

Fig. 4 Overall accuracy curves of the training and validation set of the fishing ground prediction model with multiple environmental factors at different temporal scales

of 88.74% and an F1 score of 0.8732. From the differences among the different cases, it may be observed that larger temporal scales correspond to better model performance, with the 15-day and 30-day temporal scale cases yielding favorable results. This trend aligns with the results of the fishing ground prediction model based on SST only. The variation in model performance is related to the fluctuation range of each environmental factor under different temporal scales.

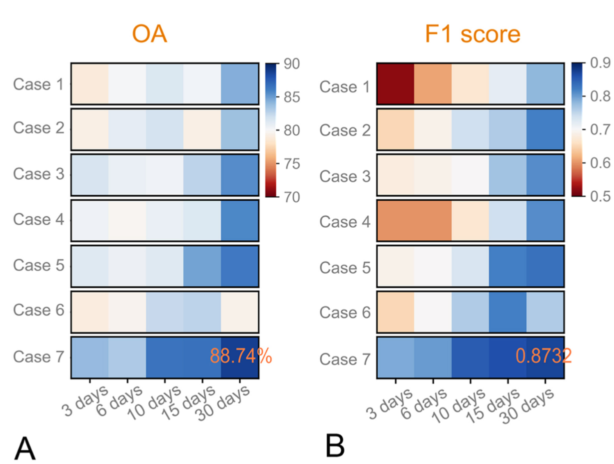

Fig. 5 Performance evaluation on the testing set of the fishing ground prediction model with multiple environmental factors at different temporal scales (OA: overall accuracy)

Prediction performance of the best case

The best performance was observed in August, with an overall accuracy (OA) of 93.59% and an F1 score of 0.9407. Conversely, the poorest performance was observed in November, with an accuracy of 81.48% and an F1 score of 0.7375 (Table 3). This result is consistent with the same time period of previous studies (Xie et al. 2024). The addition of Chl *a* resulted in a lower F1 score in November compared to previous research. This is reflected in the distribution of the center fishing ground (Fig. 6): the contour area of the center fishing ground still exhibits a latitudinal belt-shaped variation over different time periods. In the test results, the southern edge in the latitudinal direction remains relatively unchanged, whereas the northern edge shifts southward resulting in a decrease in the proportion of the center fishing ground area and a relatively narrower contour area.

Discussion

Application evaluation of fishing ground

The results obtained from the deep learning fishing ground prediction model reveal that the distribution of the center fishing ground is primarily in the form of continuous belt-shaped areas. However, actual catch data consist usually of discrete sites containing high- and low-value information. By comparing the fishing ground predicted by the deep learning model on the 2020 test dataset with the actual catch data, the application effectiveness of the model may be evaluated. This application effectiveness is likely to be closer to the real-life conditions of fishing operations, thereby improving the success rate of fishing and significantly reducing fuel costs.

Table 3 The testing results of the fishing ground prediction model with the best multiple environmental factor combination and temporal scale at each period

Period	Overall accuracy (OA, %)	Precision	Recall	F1 score
July	92.84	0.9992	0.9021	0.9482
August	93.59	0.9740	0.9095	0.9407
September	88.23	0.9972	0.8257	0.9034
October	87.55	0.9644	0.7379	0.8361
November	81.48	0.8553	0.6483	0.7375
Mean ±	88.74 ±	0.9580 ±	0.8047 ±	0.8732 ±
Standard deviation	4.35	0.0531	0.0998	0.0786

Previous data have shown that the deep learning fishing ground prediction model constructed using SST only achieved a good catch coverage rate (CCR). However, it had a high area proportion of center fishing ground (AP_{CFG}) resulting in a lower concentration level of the predicted center fishing ground. To address this, we introduced the application effect index of fishing ground (AEI_{FG}), which represents the concentration level of the center fishing ground by calculating the ratio of CCR to AP_{CFG}. We aimed to enhance the application effectiveness of the model by selecting comprehensive environmental factor combinations with high AEI_{FG} values while ensuring minimal changes in CCR. Considering that the critical environmental factor combinations may vary across different temporal periods, we chose the most suitable comprehensive environmental factor combination case based on the AEI_{FG}. The results (Table 4) showed that, except for the first half of July when no actual production data were available, the largest error occurred in the first half of November, with a CCR of 89.66%. The lowest concentration level of the center fishing ground was observed in the first half of August, with an AP_{CFG} of 64.62% and an AEI_{FG} of 1.54. By adding environmental factors, although the average CCR decreased by 0.97%, the average AP_{CFG} decreased significantly by 11.82%, whereas the average AEI_{FG} increased by 0.55. The most significant improvement in the AEI_{FG} was observed in the second half of September, which increased by 1.91. The results (Fig. 7) indicated that, during the second half of September, the actual catch data mainly concentrated in the 155°E to 165°E region of the center fishing ground. Moreover,

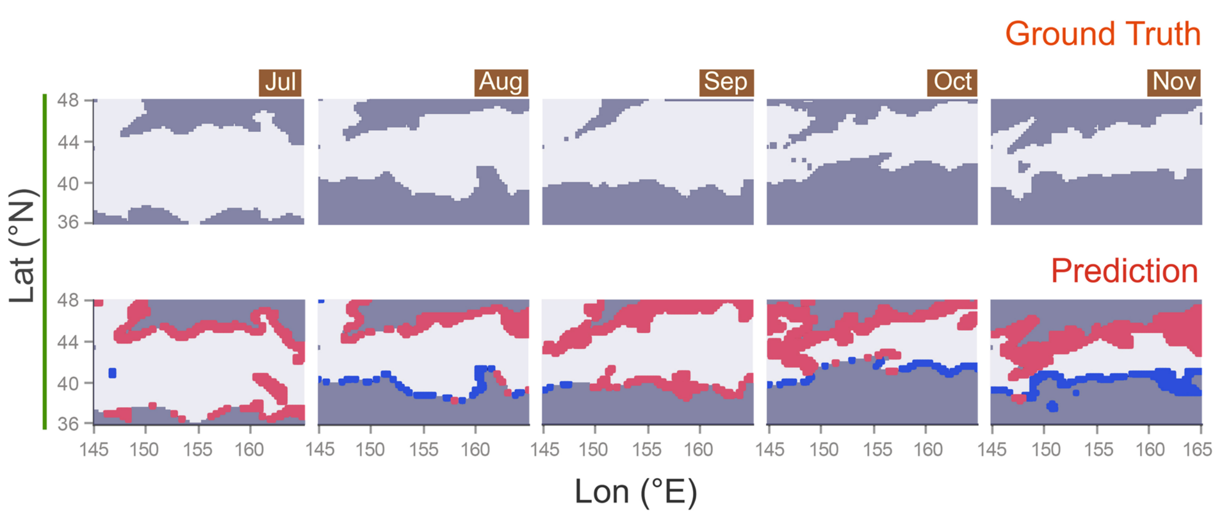

Fig. 6 Visual evaluation of the performance of the center fishing ground model in the best case (Jul, Aug, …, and Nov represent July, August, …, and November, respectively. In the ground truth, the center fishing ground and non-center fishing ground are shown in white and black, respectively. In the prediction, the correctly predicted center fishing ground and non-center fishing ground are shown in white and black, respectively; the falsely predicted center fishing ground and non-center fishing ground are shown in blue and red, respectively.)

the comprehensive environmental factor analysis significantly reduced the size of the center fishing ground west of 155°E, making it more concentrated. This period corresponds to the main fishing season of *Ommastrephes bartramii* when the catch is the largest. From the comprehensive environmental factor combination perspective, it includes all environmental factors. This indicates that the distribution of the center fishing ground during the main fishing season is primarily influenced by all environmental factors. In other temporal periods, the comprehensive environmental factor combination cases included different factors. All temporal periods contain Chl *a* except for the first half of September. This suggests that, apart from SST, Chl *a* is an important environmental factor. The importance of SSH and SSS is reflected in the different temporal periods from the beginning to the main fishing season.

The U-Net model, as one of the benchmark methods for deep learning pixel-level image classification, is characterized by its fully convolutional structure. It removes the last fully connected layer and uses upsampling layers to restore the image resolution. This makes the model more efficient and accurate in handling pixel-level image classification problems. Particularly, in this study, with the increase in environmental factors and the added complexity of the comprehensive environmental factors as output factors, the U-Net deep learning model proved to be effective. The convolutional layers in the U-Net model share weight and have local connections, which may reduce the complexity of the image feature extraction network. The U-Net model strikes a balance between exploring deep features for semantic classification and preserving high resolution, enabling better handling of pixel-level image classification tasks.

Regarding the definition of the center fishing ground, the distribution maps of each environmental factor's center fishing ground are overlayered. The regions that share the same center are defined as the center fishing ground of the comprehensive environment. This definition is more refined compared to solely using SST to define the center fishing ground. It involves making adjustments to the size of the fishing ground in the longitude direction, resulting in a more concentrated distribution of the center fishing ground. This refinement aims to improve the application effectiveness of the model.

Impact of multiple environmental factors on model performance

From the performance evaluation on the testing set of the fishing ground prediction model with multiple environmental factors at different temporal scales (Fig. 5), it may be observed that as the temporal scale increases, the model performance improves for all cases. This change occurs gradually. Since the center fishing grounds are divided based on the range of environmental factors, when the temporal scale is smaller, the environmental factors fluctuate more intensely over the time series. Moreover, the range of comprehensive environmental factors under the superposition of these factors also exhibits more complex and intense fluctuations. Previous research has shown that in the performance of fishing ground prediction models constructed using only SST, cases with temporal scales of 3 and 6 days have poorer performance. In this study, Case 1, which includes all combinations of environmental factors, had the lowest OA and F1 scores at a temporal scale of 3 days, with values of 78.86% and 0.5249, respectively. The performance of Case 1 was

Table 4 Comparison of the application evaluation of actual catch data on the testing set on the center fishing ground prediction model with single-factor and multi-factor combinations

Period	Catch coverage rate (CCR, %)		Area proportion of center fishing ground (AP_{CFG}, %)		Application effect index of fishing ground (AEI_{FG})		Multi-factor combination case
	Single factor	Multiple factors	Single factor	Multiple factors	Single factor	Multiple factors	
July (1st half)	/	/	/	/	/	/	/
July (2nd half)	100.00	100.00	72.42	48.40	1.38	2.06	SST + SSH + Chl *a*
August (1st half)	99.40	98.44	64.62	61.91	1.54	1.59	SST + Chl *a*
August (2nd half)	97.93	96.78	50.74	44.29	1.93	2.19	SST + SSS + Chl *a*
September (1st half)	100.00	97.53	56.09	42.15	1.78	2.31	SST + SSH
September (2nd half)	100.00	98.15	65.36	28.57	1.53	3.44	SST + SSH + SSS + Chl *a*
October (1st half)	100.00	99.84	37.39	32.62	2.67	3.06	SST + Chl *a*
October (2nd half)	100.00	100.00	40.05	30.43	2.49	3.28	SST + Chl *a*
November (1st half)	89.66	87.48	44.06	37.68	2.03	2.32	SST + SSS + Chl *a*
November (2nd half)	100.00	100.00	49.60	47.91	2.01	2.08	SST + Chl *a*
Mean	98.55	97.57	53.37	41.55	1.93	2.48	

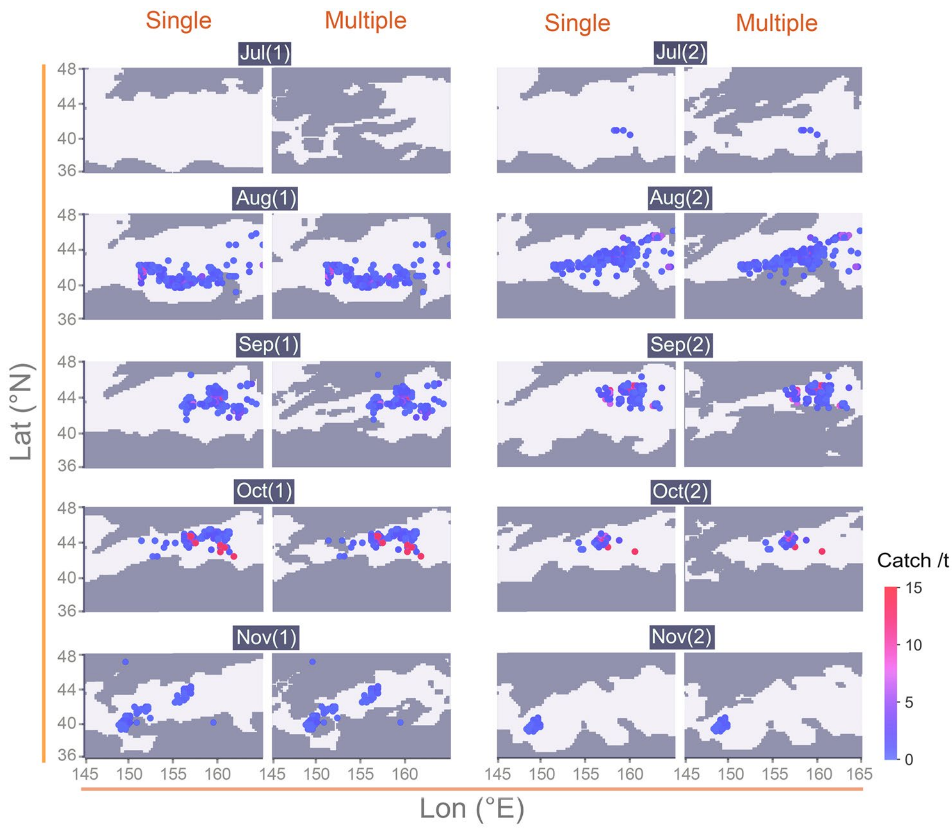

Fig. 7 Comparison of actual catch data superimposed onto the predicted results on single factor and the best AEI_{FG} index multi-factor fishing ground prediction model (single and multiple indicate single-factor and multi-factor combination models, respectively. The predicted center fishing ground is illustrated in white, the predicted non-center fishing ground in black, and the actual catch data as colored dots.)

significantly lower than that constructed using only SST. This suggests that when the environmental field becomes more complex and fluctuations become more intense, fewer environmental factors lead to better model performance. From Case 2 to 7, the comprehensive environmental factor combination cases involve the removal of 1 or 2 environmental factors. Compared to Case 1, these cases showed an improvement in model performance to some extent. Among them, Case 7, which includes SST and Chl *a*, exhibited the most significant improvement in model performance. The results at a temporal scale of 3 days were even better than the results of the models at a temporal scale of 30 days in other cases. From the perspective of the range of changes in each environmental factor (Fig. 8), the reasons might be that SST and Chl *a* exhibit more pronounced seasonal trends, and the coupling between the two factors is better in terms of temporal sequences. However, the addition of SSH or SSS factors reduces the compatibility between the environmental factors, resulting in a negative impact on the model's performance. When the temporal scale is 15 days and 30 days, all combinations of comprehensive environmental factors perform well as the fluctuations in each environmental factor are relatively smooth, with OA above 79.00% and F1 scores above 0.7200. The optimal results are observed in the 30-day temporal scale of fishing ground prediction, indicating better compatibility in fisheries oceanography and deep learning at this temporal scale. In recent years, with the update of fishing vessels and other fishing equipment in fisheries production, a finer temporal scale is sometimes required. To strike a balance between model results and actual fisheries catch, it is possible to select a more refined temporal scale case within the acceptable range of model accuracy requirements.

Importance of each environmental factor on the fishing ground distribution

As a representative of short-lived species in the Northwest Pacific, the lifecycle of *Ommastrephes bartramii* spans approximately 1 year. Therefore, its life-history processes are highly sensitive to variations in the marine environment. During different periods, the population of *Ommastrephes bartramii* exhibits varying ranges of suitability to different environmental factors, and there are significant seasonal variations (Yu et al. 2016). Due to the diverse temporal changes in each environmental factor, the optimal ranges of these factors for *Ommastrephes bartramii* also differ. Therefore, analyzing the temporal variations in each environmental factor in relation to the corresponding center fishing ground is crucial for understanding their importance in influencing the center fishing ground.

Sea surface temperature (SST) is the most crucial marine environmental factor affecting the fishing ground

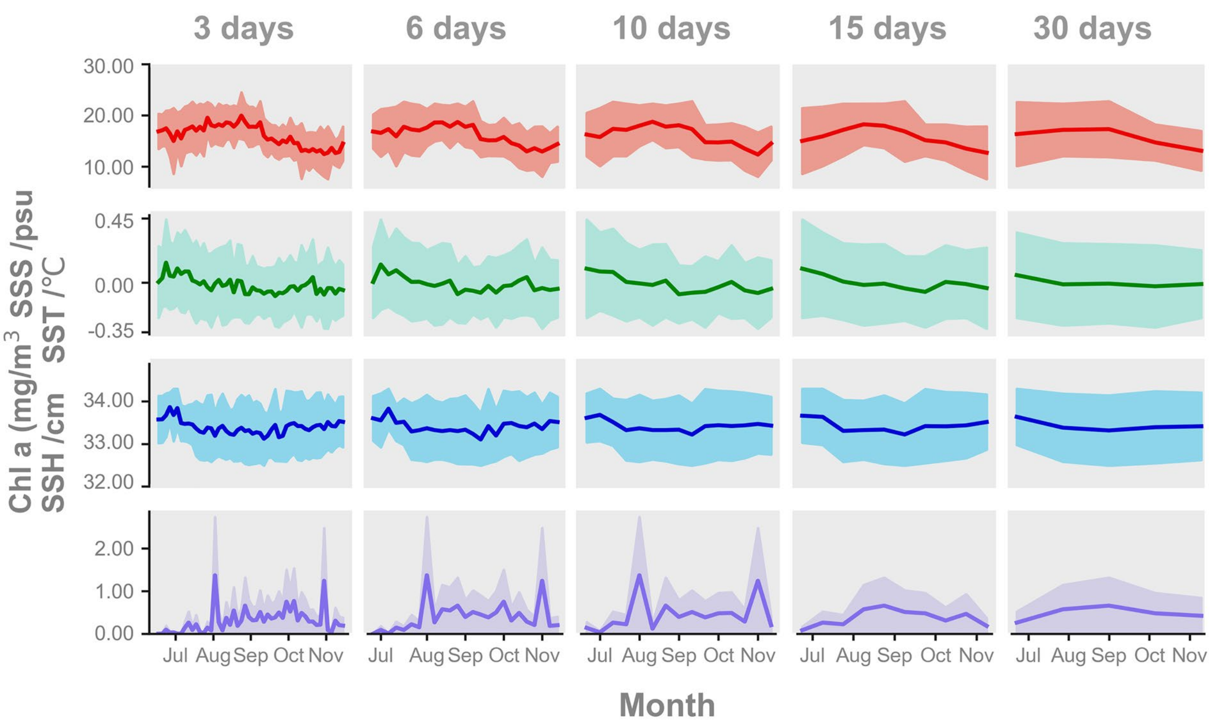

Fig. 8 Variation in each environmental factor range in center fishing ground of *Ommastrephes bartramii* in different temporal cases

distribution of pelagic economic species (Lajus et al. 2021; Suca et al. 2022). The suitable SST range for *Ommastrephes bartramii* exhibits significant seasonal variations each month (Chen 2006). Additionally, the distribution of the center fishing ground experiences significant interannual variations influenced by climate events, such as El Niño and La Niña (Alabia et al. 2016b; Yu et al. 2019). The center fishing ground is primarily characterized by a belt-shaped distribution with temporal variations in latitude and changes in area size. The gravity of the center fishing ground shifts northward and then southward, with the smallest area and highest concentration observed in October. This pattern corresponds strongly to the north–south displacement of SST isotherms, and the center fishing ground does not appear in regions with excessively low or high SST (Fig. 9A).

Sea surface height (SSH) contains information about ocean dynamics, including ocean currents, tides, water masses, and mesoscale eddies. They play a significant role in fishing grounds (Yatsu et al 2000). Eddy regions induce intense vertical movement of seawater, promoting mixing and exchange of nutrients between the upper and lower layers. This leads to an increase in marine plankton, which serves as food for fish, thus favoring the formation of fishing grounds (Fan et al. 2009; Hardman-Mountford et al. 2003). Previous studies have indicated that the center fishing ground of *Ommastrephes bartramii* is mainly distributed along the edges of eddies, with a higher abundance of warm eddies compared to cold eddies (Zhang et al. 2022). Regarding the temporal variation in SSH distribution, seasonal changes are not prominent. The maximum and minimum values of SSH correspond to the centers of eddies, which are mostly non-center fishing grounds and exhibit a high degree of correlation. In the comprehensive environmental factor model, the impact of SSH on the distribution of the center fishing ground is primarily to reduce the area of some eddy centers within the belt-shaped distribution established using the SST. This refinement enhances the precision of the fishing ground distribution (Fig. 9B).

Sea surface salinity (SSS) and chlorophyll *a* (Chl *a*) are important factors in the formation of primary producers, phytoplankton. They directly influence the structure and functionality of marine ecosystems, thus exerting a decisive impact on the formation of fishing grounds (Fan et al. 2009; Mustapha et al. 2009). Previous research has shown (Alabia et al. 2015) that the fishing ground distribution of *Ommastrephes bartramii* is on the warm side of the convergence zone between cold, low-salinity water and warm, high-salinity water tongues within oceanic frontal regions. The results of this study (Fig. 9C) are consistent with previous research findings. The impact of SSS on the distribution of the center fishing ground is to reduce the area of the cold, low-salinity oceanic frontal region in the northwest direction. Unlike other environmental factors, Chl *a* has a large number of missing values. Previous data have shown that higher catch is associated with lower Chl *a* levels (Yu et al. 2017). Therefore, the impact of Chl *a* on the distribution of the center

Fig. 9 Variation in environmental factors with corresponding center fishing ground monthly (**A** for SST, **B** for SSH, **C** for SSS, and **D** for Chl *a*)

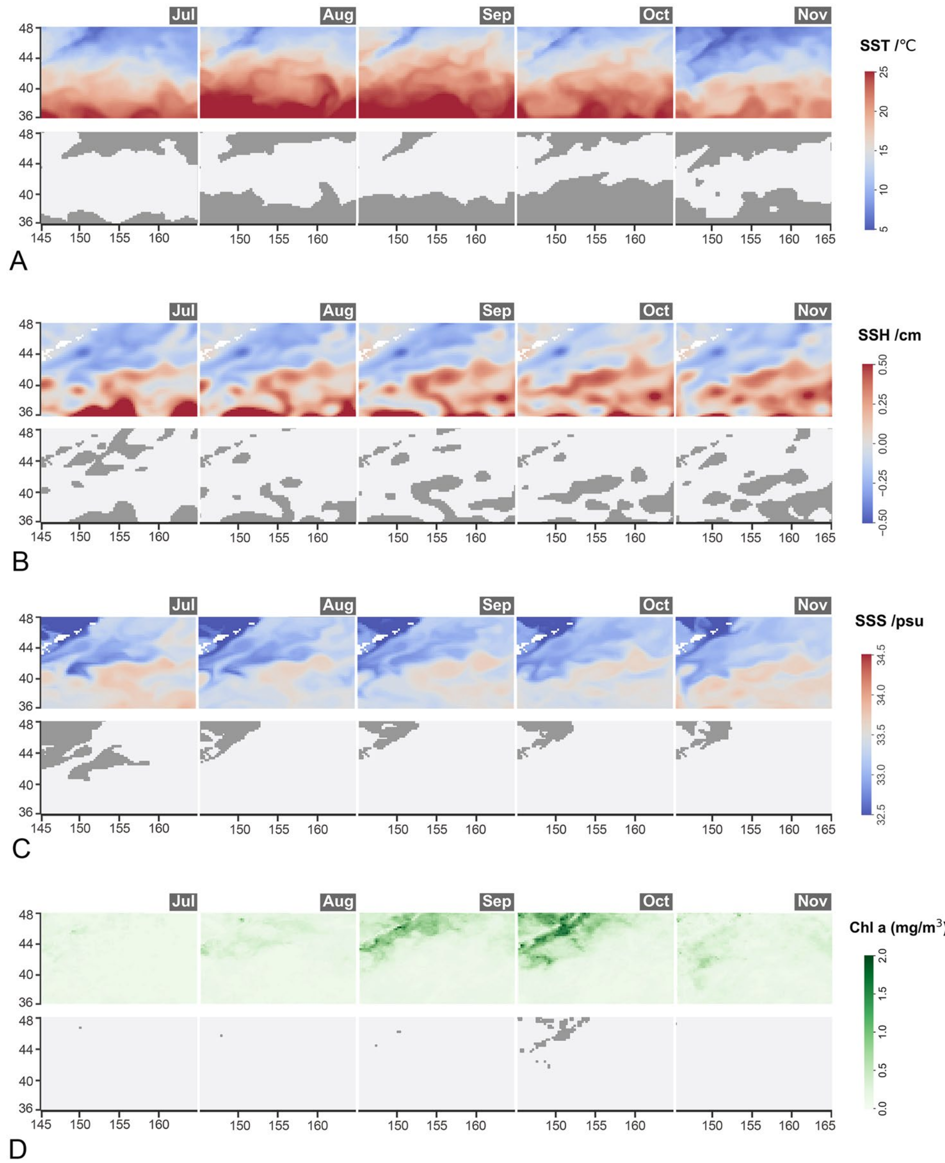

fishing ground is minimal. When higher values of Chl *a* are present, it reduces the area of the center fishing ground in that region. However, this reduction in area is much smaller compared to other environmental factors (Fig. 9D). This may explain why the comprehensive environmental factor model including SST and Chl *a* performs the best. The inclusion of Chl *a* only provides minor adjustments to the model results based on the SST, resulting in results that are close to those of the single-factor SST model. However, in terms of the application evaluation of fishing grounds, Chl *a* is not more significant than other environmental factors.

Conclusions

In this study, we proposed a deep learning-based fishing ground prediction method with multiple environmental factors. Through the analysis of results from different temporal scales and environmental factor combinations, we found that the optimal temporal scale is 30 days, and the combination of factors includes SST and Chl *a*. The larger the temporal scale, the more stable and accurate the model performance. We introduced the application effect index of the fishing ground (AEI_{FG}) to address the issue of excessive fishing ground area and low concentration when using single-factor prediction. By incorporating different environmental factor combinations in different temporal periods, we successfully improved the application effectiveness of fishing ground prediction and achieved more accurate results.

However, there are some limitations in the selection of environmental factors and the quality of data sources in this study. Future research could focus on selecting a greater number of more important and higher quality environmental factors, and optimizing the model's performance by incorporating oceanic climate events. Additionally, it is noteworthy that this study did not utilize the specific information and attributes of the *Ommastrephes bartramii* fishing ground in the Northwest Pacific Ocean. Therefore, the research method and approach proposed in this paper may be applied to other fishing grounds of species as well.

Acknowledgements The work is supported in part by the National Natural Science Foundation of China under Grant 41876141 and Grant 42006159, and in part by the National Key R&D Programme of China under Grant 2019YFD0901404. The authors thank the Chinese Squid-Jigging Technology Group at Shanghai Ocean University for providing the fishery data. The authors thank the National Oceanic and Atmospheric Administration and the University of Hawaii for providing the environmental data.

Author contributions XJC and BL conceived the idea. MYX carried out the experiments and wrote the manuscript. BL and XJC revised the manuscript. All authors contributed to the article and approved the submitted version.

Data availability The fishery data are not available for sharing at the request of the copyright holder. The environmental factor data used in this study are available from OceanWatch of the National Oceanic and Atmospheric Administration and the University of Hawaii. Users can download these data from online services (https://oceanwatch.pifsc.noaa.gov/erddap/griddap/CRW_sst_v1_0.html; http://apdrc.soest.hawaii.edu/data) for free.

Declarations

Conflict of interest We, i.e., all the authors, have no conflicts of interest to disclose.

Animal and human rights statement No human or animal subjects were used during the course of this research.

References

Alabia ID, Saitoh SI, Mugo R, Igarashi H, Ishikawa Y, Usui N, Kamachi M, Awaji T, Seito M (2015) Seasonal potential fishing ground prediction of neon flying squid (*Ommastrephes bartramii*) in the western and central North Pacific. Fish Oceanogr 24:190–203

Alabia ID, Saitoh SI, Igarashi H, Ishikawa Y, Usui N, Kamachi M, Awaji T, Seito M (2016a) Future projected impacts of ocean warming to potential squid habitat in western and central North Pacific. ICES J Mar Sci 73:1343–1356

Alabia ID, Saitoh SI, Hirawake T, Igarashi H, Ishikawa Y, Usui N, Kamachi M, Awaji T, Seito M (2016b) Elucidating the potential squid habitat responses in the central North Pacific to the recent ENSO flavors. Hydrobiologia 772:215–227

Allken V, Rosen S, Handegard NO, Malde K (2021) A deep learning-based method to identify and count pelagic and mesopelagic fishes from trawl camera images. ICES J Mar Sci 78:3780–3792

Chande MA, Mgaya YD, Benno LB, Limbu SM (2021) The influence of environmental variables on the abundance and temporal distribution of Octopus cyanea around Mafia Island. Tanzania Fish Res 241:105991

Chen XJ (2006) The catch distribution of *Ommastrephes batramii* in squid jigging fishery and the relationship between fishing ground and SST in the North Pacific Ocean in 2004. Mar Sci B 8:83–91

Chen XJ (2022) Theory and method of fisheries forecasting. Springer Nature, Singapore

Chen XJ, Liu BL, Chen Y (2008) A review of the development of Chinese distant-water squid jigging fisheries. Fish Res 89:211–221

Chen BH, Bai YL, Wang JY, Ke QZ, Zhou ZX, Zhou T, Pan Y, Wu RX, Wu XF, Zheng WQ, Xu P (2023) Population structure and genome-wide evolutionary signatures reveal putative climate-driven habitat change and local adaptation in the large yellow croaker. Mar Life Sci Tech 5:141–154

Fan W, Wu YM, Cui XS (2009) The study on fishing ground of neon flying squid, *Ommastrephes bartramii*, and ocean environment based on remote sensing data in the Northwest Pacific Ocean. Chin J Oceanol Limn 27:408

Gao KS, Gao G, Wang YJ, DuPont S (2020) Impacts of ocean acidification under multiple stressors on typical organisms and ecological processes. Mar Life Sci Tech 2:279–291

Hardman-Mountford NJ, Richardson AJ, Boyer DC, Kreiner A, Boyer HJ (2003) Relating sardine recruitment in the Northern Benguela to satellite-derived sea surface height using a neural network pattern recognition approach. Prog Oceanogr 59:241–255

Huang HC, Yang JP, Huang SX, Gu BW, Wang Y, Wang L, Jiao NZ, Xu DP (2021) Spatial distribution of planktonic ciliates in the western Pacific Ocean: along the transect from Shenzhen (China) to Pohnpei (Micronesia). Mar Life Sci Tech 3:103–115

Kroodsma DA, Mayorga J, Hochberg T, Miller NA, Boerder K, Ferretti F, Wilson A, Bergman B, White TD, Block BA, Woods P, Sullivan B, Costello C, Worm B (2018) Tracking the global footprint of fisheries. Science 359:904–908

Lajus D, Ivanova T, Rybkina E, Lajus J, Ivanov M (2021) Multidecadal fluctuations of threespine stickleback in the White Sea and their correlation with temperature. ICES J Mar Sci 78:653–665

Landy JC, Dawson GJ, Tsamados M, Bushuk M, Stroeve JC, Howell SE, Krumpen T, Babb DG, Komarov AS, Heorton HBS, Belter HJ, Aksenov Y (2022) A year-round satellite sea-ice thickness record from CryoSat-2. Nature 609:517–522

Lei L (2016) Remote sensing of marine fisheries. China Ocean Press, Beijing, China

Li XF, Liu B, Zheng G, Ren YB, Zhang SS, Liu YJ, Gao L, Liu YH, Zhang B, Wang F (2020) Deep-learning-based information mining from ocean remote-sensing imagery. Natl Sci Rev 7:1584–1605

Lin TY, Goyal P, Girshick R, He K, Dollár P (2017) Focal loss for dense object detection. In Proceedings of the IEEE International Conference on Computer Vision pp: 2980–2988

Liu B, Li XF, Zheng G (2019) Coastal inundation mapping from bi-temporal and dual-polarization SAR imagery based on deep convolutional neural networks. J Geophys Res: Oceans 124:9101–9113

Liu GY, Liu B, Zheng G, Li XF (2022) Environment monitoring of Shanghai Nanhui intertidal zone with dual-polarimetric SAR data based on deep learning. IEEE T Geosci Remote 60:1–18

Mustapha MA, Sei-Ichi S, Lihan T (2009) Satellite-measured seasonal variations in primary production in the scallop-farming region of the Okhotsk Sea. ICES J Mar Sci 66:1557–1569

Reichstein M, Camps-Valls G, Stevens B, Jung M, Denzler J, Carvalhais N (2019) Deep learning and process understanding for data-driven Earth system science. Nature 566:195–204

Ronneberger O, Fischer P, Brox T (2015) U-net: convolutional networks for biomedical image segmentation. In: Navab N, Hornegger J, Wells W, Frangi A (eds) Medical image computing and computer-assisted intervention – MICCAI 2015. MICCAI 2015. Lecture Notes in Computer Science. pp 234–241

Skogen MD, Hjøllo SS, Sandø AB, Tjiputra J (2018) Future ecosystem changes in the Northeast Atlantic: a comparison between a global and a regional model system. ICES J Mar Sci 75:2355–2369

Song LM, Ren SY, Zhang M, Sui HS (2022) Fishing ground forecasting of bigeye tuna (*Thunnus obesus*) in the tropical waters of Atlantic Ocean based on ensemble learning. J Fish China 47:64–76 (**in Chinese with English abstract**)

Suca JJ, Santora JA, Field JC, Curtis KA, Muhling BA, Cimino MA, Hazen EL, Bograd SJ (2022) Temperature and upwelling dynamics drive market squid (*Doryteuthis opalescens*) distribution and abundance in the California Current. ICES J Mar Sci 79:2489–2509

Tian SQ, Chen XJ, Chen Y, Xu LL, Dai XJ (2009) Standardizing CPUE of *Ommastrephes bartramii* for Chinese squid-jigging fishery in Northwest Pacific Ocean. Chin J Oceanol Limn 27:729–739

Tompson J, Goroshin R, Jain A, LeCun Y, Bregler C (2015) Efficient object localization using convolutional networks. In Proceedings of the IEEE Conference on Computer Vision and Pattern Recognition pp 648–656

Xie MY, Liu B, Chen XJ, Yu W, Wang JT (2024) Deep learning-based fishing ground prediction using asymmetric spatiotemporal scales: A case study of *Ommastrephes bartramii*. Fishes 9:64

Yatsu A, Watanabe T, Mori J, Nagasawa K, Ishida Y, Meguro T, Kamei Y, Sakurai Y (2000) Interannual variability in stock abundance of the neon flying squid, *Ommastrephes bartramii*, in the North Pacific Ocean during 1979–1998: impact of driftnet fishing and oceanographic conditions. Fish Oceanogr 9:163–170

Yu W, Yi Q, Chen XJ, Chen Y (2016) Modeling the effects of climate variability on habitat suitability of jumbo flying squid, *Dosidicus gigas*, in the Southeast Pacific Ocean off Peru. ICES J Mar Sci 73:239–249

Yu W, Chen XJ, Yi Q (2017) Fishing ground distribution of neon flying squid (*Ommastrephes bartramii*) in relation to oceanographic conditions in the northwest Pacific Ocean. J Ocean U China 16:1157–1166

Yu W, Chen X, Zhang Y, Yi Q (2019) Habitat suitability modeling revealing environmental-driven abundance variability and geographical distribution shift of winter-spring cohort of neon flying squid *Ommastrephes bartramii* in the northwest Pacific Ocean. ICES J Mar Sci 76:1722–1735

Zhang YC, Yu W, Chen XJ, Zhou M, Zhang CL (2022) Evaluating the impacts of mesoscale eddies on abundance and distribution of neon flying squid in the Northwest Pacific Ocean. Front Mar Sci. https://doi.org/10.3389/fmars.2022.862273

Zheng G, Li X, Zhang RH, Liu B (2020) Purely satellite data–driven deep learning forecast of complicated tropical instability waves. Sci Adv 6:eaba1482